Available online at www.sciencedirect.com

ScienceDirect

Ceramics International 40 (2014) 4367–4373

CERAMICS INTERNATIONAL

www.elsevier.com/locate/ceramint

Colour performance investigation of a Cr_2O_3 green pigment prepared via the thermal decomposition of CrOOH

Shu-ting Liang[a,b,c,d], Hong-ling Zhang[a,b,c,*], Min-ting Luo[a,b,c], Ke-jun Luo[e], Ping Li[a,b,c], Hong-bin Xu[a,b,c], Yi Zhang[a,b,c]

[a]*Institute of Process Engineering, Chinese Academy of Sciences, Beijing 100190, China*
[b]*Key Laboratory of Green Process and Engineering, Chinese Academy of Sciences, Beijing 100190, China*
[c]*National Engineering Laboratory for Hydrometallurgical Cleaner Production Technology, Beijing 100190, China*
[d]*Graduate University of Chinese Academy of Sciences, Beijing 100190, China*
[e]*Bluestar Yima Chrome Chemical Materials Co. Ltd., Yima 472300, China*

Received 5 July 2013; received in revised form 24 August 2013; accepted 26 August 2013
Available online 5 September 2013

Abstract

In this study, Cr_2O_3 green pigments were prepared using two types of CrOOH, α-CrOOH and γ-CrOOH, and the resulting pigments were characterised. The thermal decomposition behaviours of the two types of synthesised CrOOH were discussed. The resulting Cr_2O_3 pigments were characterised using X-ray diffraction (XRD), scanning electron microscope (SEM), International Commission on Illumination (CIE-$L^*a^*b^*$) and ultraviolet–visible diffuse reflectance spectroscopy (UV–vis DRS). The key factors and mechanism that influenced the preparation of the Cr_2O_3 green pigments were studied. The results revealed that γ-CrOOH produces Cr_2O_3 that is more homogeneous, has a uniform size of 200–400 nm and a yellowish-green colour compared to α-CrOOH, which produces Cr_2O_3 with non-uniform sizes and a brownish-green colour. In addition to the different particle morphologies and sizes, the change in the crystal field, which leads to a shift in the $^4A_{2g} \rightarrow {}^4T_{1g}$ and $^4A_{2g} \rightarrow {}^2T_{2g}$ transition, also affects the colour of the pigment. Lastly, a series of Cr_2O_3 green pigments displaying a wide range of colours were prepared by calcining mixtures of α-CrOOH and γ-CrOOH with different compositions.

Keywords: Chrome oxide green pigment; Chromium oxyhydroxide; Colour performance; Green processing

1. Introduction

Pigments are the primary ancillary materials used in the production of paints, plastics, rubber, building materials, and inks. Due to the different special requirements of various applications for pigments, such as coatings, inks, and ceramics, a general pigment cannot satisfy the requirements for all cases. Therefore, researchers are committed to the development of special types of pigments. Chrome oxide (Cr_2O_3) is known as one of the most desirable green pigments due to its high thermal stability, migration resistance, and excellent light fastness [1]. Colour performance is the most important requirement for Cr_2O_3 pigments. However, the chromatic properties of Cr_2O_3 pigments are limited to one colour and unsatisfactory. Extensive research works have been devoted to producing the widest range of pigment-grade Cr_2O_3 on the market while maintaining its thermal and chemical stabilities.

At present, the industrial production of Cr_2O_3 green pigment employs two conventional techniques: one is the reduction of alkali metal chromate with ammonium sulphate, sulphur or carbon; the other is the thermal decomposition of Cr(VI)-compounds [2–4]. Numerous attempts have been devoted to synthesising different colours of Cr_2O_3 using conventional techniques. These attempts can be classified into two approaches. One approach is adding additives. Additives would have to produce controlled growth because crystal size and uniformity determine the pigment characteristics of Cr_2O_3. Several compounds, such as sawdust, starch, sodium sulphate, and boric acid, have been used as additives. This method converts less green, less yellow, and darker Cr_2O_3 to a more valuable bright green Cr_2O_3 [5–7]. The other

*Corresponding author at: Institute of Process Engineering, Chinese Academy of Sciences, Beijing 100190, China. Tel.: +86 10 82544808; fax: +86 10 82544808.
E-mail address: hlzhang@home.ipe.ac.cn (H.-l. Zhang).

0272-8842/$ - see front matter © 2013 Elsevier Ltd and Techna Group S.r.l. All rights reserved.
http://dx.doi.org/10.1016/j.ceramint.2013.08.107

approach is doping other metal ions into Cr_2O_3 to form solid solutions. Several metal ions, such as Al, Ba [8], Ti, V [9,10], La, Pr [11], Co [12,13], Fe [14], Y, and Mg [15], have been doped into Cr_2O_3 to replace the chromophore ion and to strengthen the colour. However, for the traditional production process, the environmental pollution resulting from sulphur dioxide and Cr(VI)-containing dusts is often serious [16,17]. In addition, the amounts of the other metal ions must be strictly controlled because they may be able to reduce the main content of Cr_2O_3 pigments.

A novel process for preparing Cr_2O_3 from chromite ore has recently been developed in our laboratory. First, chromite ore was decomposed by a high concentration of a KOH aqueous solution under an oxidative atmosphere to obtain potassium chromate (K_2CrO_4) [18–20]. The obtained K_2CrO_4 was then converted into chromium oxyhydroxides (CrOOH) through hydrogen reduction [21]. Lastly, Cr_2O_3 was obtained through the thermal decomposition of CrOOH [22]. This new method greatly decreased the environmental pollution resulting from sulphur dioxide and Cr(VI)-containing dusts. Although these Cr_2O_3 products exhibit rather good tinting strength and thermal stability, their chromatic properties are single and unsatisfactory. Therefore, further studies are needed to produce the widest range of pigment-grade Cr_2O_3.

Thus, this work was aimed at increasing the diversity of Cr_2O_3 colours and preparing a series of Cr_2O_3 based on the thermal decomposition of CrOOH. It is well known that CrOOH is the primary precursor for the preparation of chromium oxides (Cr_2O_3, CrO_2) [23–26]. Three synthetic types of CrOOH have been reported to date. The first is rhombohedral α-CrOOH with space group R3m; the second is orthorhombic β-CrOOH with space group Pnnm; and the third is amorphous γ-CrOOH [27–30]. However, few studies have reported using the thermal decomposition of CrOOH to manufacture Cr_2O_3 green pigments in industry. The present work is focused on synthesising Cr_2O_3 pigments by calcining two types of CrOOH. γ-CrOOH and α-CrOOH were here prepared from the hydrogen reduction of K_2CrO_4. The influence of different thermal decompositions of γ-CrOOH and α-CrOOH on the crystallisation, morphology, and colour performance of Cr_2O_3 was studied. Lastly, a series of pigments were synthesised by calcining mixtures of α-CrOOH and γ-CrOOH with different compositions. The characteristics of Cr_2O_3 with different colours were discussed. The key factors and mechanism that influence the colour were analysed.

2. Experimental

The K_2CrO_4 used in this work was of analytical grade and was manufactured via the novel KOH hydrometallurgical process [20]. A demonstration plant (Bluestar Yima Chrome Chemical Materials Co. Ltd.) which uses this process was built in He'nan Province, PR China. The purity of the hydrogen gas was 99.99% v/v.

Gas–solid reduction was performed in a tube furnace with a programmable temperature controller. A nickel boat, loaded with 60 g of K_2CrO_4, was placed into the furnace tube. Hydrogen was introduced into the tube at a flow rate of 0.6 L/min. The reaction temperature was increased to and maintained at 450 °C for 1 h. After the tube furnace was cooled, the reduction product was lixiviated many times with distilled water to remove soluble components. After filtering, the remaining solid intermediate in the form of amorphous CrOOH was then dried. The colour of the filtrate was also observed to change from the previous green-yellow colour to yellow after it was completely diluted, and a type of green gel material in the form of $Cr(OH)_3 \cdot 3H_2O$ appeared in the solution [21].

When the hydrogen reduction temperature was increased to 650 °C, it was rather difficult to form $Cr(OH)_3 \cdot 3H_2O$ [21]. The reduction products obtained at 650 °C were lixiviated with distilled water to remove soluble components. After filtering, the remaining solid intermediate was added to distilled water, which was maintained under constant stirring for more than 12 h at 80 °C. Some greyish-green powdered substances were observed to be suspended in solution, while large black particles settled at the bottom of the beaker. The large black particles and the greyish-green powder were separated by centrifugation, dried at 100 °C for 12 h, and then named samples S1 and S2, respectively.

Samples S1 and S2 were sintered in an electric muffle furnace at 950 °C for a soaking time of 1.5 h and then rapidly cooled. The resulting Cr_2O_3 samples were lixiviated with distilled water. The final products were recovered, generally by filtration and drying.

The colour performance data were reported using the CIE $L^*a^*b^*$ (1976) colourimetric system. The CIE-$L^*a^*b^*$ colour parameters were measured for the Cr_2O_3 samples and for standard samples used in industries. A Datacolor 110 colorimeter, manufactured by Datacolor Co., Ltd., USA, equipped with an illuminant D65 and 10° complementary observer as required, was employed. The value of CIE-L^* denotes the degree of lightness and darkness of the colour in relation to the scale extending from white ($L^*=100$) to black ($L^*=0$). The value of CIE-a^* denotes the scale extending from the green ($-a^*$) to red ($+a^*$) axes. The value of CIE-b^* denotes the scale extending from the blue ($-b^*$) to yellow ($+b^*$) axes. For each colourimetric parameter of the analysed sample, three values were measured, and the average value was chosen as the measurement result.

Thermogravimetry (TG) and differential scanning calorimetry (DSC) measurements were performed in an air atmosphere at a heating rate of 10 °C/min. Microstructural characterisation of the powders was conducted using a JSM-6700F NT scanning electron microscope (SEM), supplied by JEOL. X-ray diffraction (XRD) patterns were recorded using a Rigaku diffractometer employing Cu Ka radiation (from 5° to 90° 2θ, with steps of 0.02° 2θ, and a counting time of 2 s per step). The optical properties of the samples were then analysed by diffuse reflectance spectroscopy (UV–vis), which was performed using a Perkin-Elmer (lambda 2000) spectrophotometer in the wavelength range of 400–780 nm employing barium sulphate as a reference.

3. Results and discussion

XRD was used to determine the crystal structure of the products. Fig. 1 presents typical XRD patterns of sample S1 (the large black particles) and sample S2 (the greyish-green powdered substances)

obtained by hydrolysing the solid intermediates. Sample S1 presents an amorphous phase, which coincides with amorphous γ-CrOOH. Compared to sample S1, all diffraction peaks in sample S2 are well indexed and in good agreement with the standard JCPDF card no. 090331. No impurity peaks are observed, indicating that sample S2 has a single crystalline phase: rhombohedral α-CrOOH [31]. As reported by Li et al., the intermediate products that were obtained from the high hydrogen reduction temperature (650 °C) are a well-crystallised material [22]. The XRD measurement results indicate that the CrOOH in sample S1 is amorphous (γ-CrOOH), while the CrOOH in sample S2 is rhombohedral (α-CrOOH).

Fig. 2 compares the SEM images of samples S1 and S2. As shown in Fig. 2(a), sample S1 appears to be non-crystallised lumpy aggregates. A similar SEM morphology of natural γ-CrOOH was reported by Shpachenko et al. when they investigated the genesis and compositional characteristics of natural γ-CrOOH [30]. Sample S2 is observed to have a crystallised plate-like morphology, as shown in Fig. 2(b). Some of the particles have the shape of a hexagonal crystal platelet, as expected from the R3m crystal structure, which is consistent with previous studies [23].

The TG-DSC analyses of γ-CrOOH and α-CrOOH are shown in Fig. 3. A minor mass loss step is observed from 25 °C to 430 °C, which is attributed to the loss of water from the structure. A second mass loss step is observed between 420 and 440 °C, which is attributed to the dehydroxylation of the compound. A Cr_2O_3 crystalline phase is produced from the thermal decomposition of CrOOH. Amorphous γ-CrOOH shows a sharp exothermic peak centred at 437.1 °C corresponding to the crystallisation of Cr_2O_3, whereas α-CrOOH shows an endothermic peak centred at 426.3 °C corresponding to the crystallisation of Cr_2O_3. The reactions are described as follows:

$$2\gamma\text{-CrOOH} = Cr_2O_3 + H_2O \quad (1)$$

$$2\alpha\text{-CrOOH} = Cr_2O_3 + H_2O \quad (2)$$

During the course of decomposition, a particle was first destroyed into fine Cr_2O_3 crystallites, accompanied by micropore formation, and recrystallised to yield a single crystal Cr_2O_3 particle [32]. The unit cell parameters of α-CrOOH are $a=b=2.979$ Å and $c=13.70$ Å. The α-CrOOH is a layered structure compound, in which the linked CrO_6^{9-} plates are stacked in the c-direction through H-bonding [31]. During the decomposition of α-CrOOH, the water molecules to be emitted will be formed by heat from all of the hydrogen atoms in the hydrogen atom layers and one-fourth of the oxygen atoms in two oxygen atom layers. One-fourth of the chromium ions in two chromium ion layers must be displaced into the hydrogen atom layers [32,33]. This course would absorb heat and requires more energy than the decomposition process of amorphous γ-CrOOH. Therefore, α-CrOOH shows an endothermic peak. However, the crystallisation of Cr_2O_3 is an exothermic process. Therefore, amorphous γ-CrOOH shows a sharp exothermic peak. Li et al. also reported that under a high hydrogen reduction temperature, the intermediate would require more energy to form Cr_2O_3 [22]. The result is consistent with previous reports.

During the thermal decomposition of CrOOH up to 950 °C, all samples are observed to transform into a well-crystalline Cr_2O_3 phase, as shown in Fig. 4. Cr_2O_3 with space group R-3c is identified according to JCPDS card No. 38-1479. All of these thermal products are observed to have high crystallinity. No impurity peaks are observed.

Fig. 5 compares the morphologies of Cr_2O_3 samples obtained by calcining different precursors. According to Fig. 5(a), the particles of sample A1 (prepared from γ-CrOOH) exhibit regular tabular

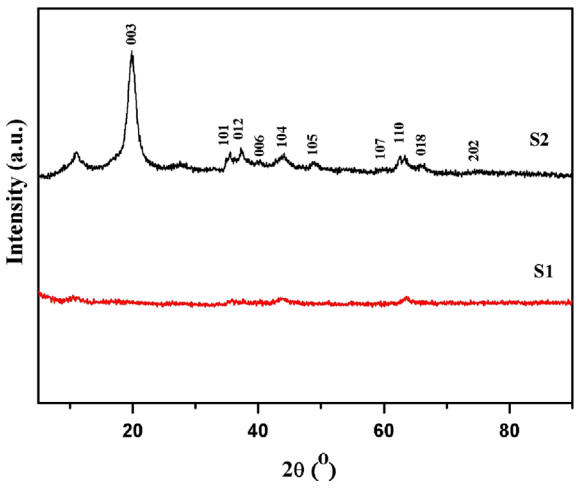

Fig. 1. XRD patterns of samples S1 and S2.

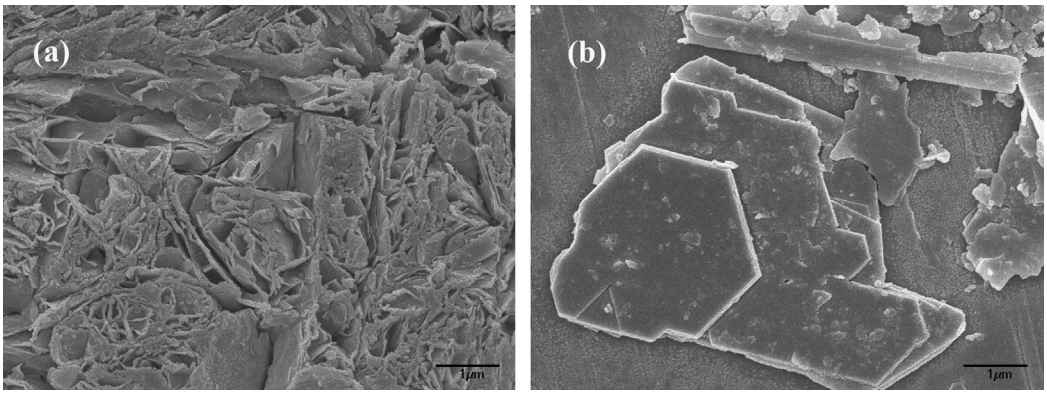

Fig. 2. SEM of samples S1 and S2: (a) S1; (b) S2.

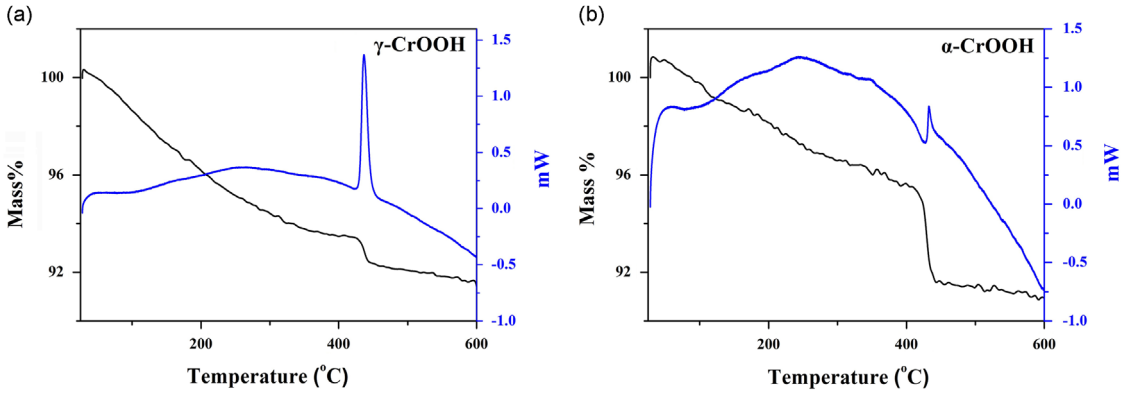

Fig. 3. TG-DSC curves of CrOOH precursors in air: (a) γ-CrOOH; (b) α-CrOOH.

morphologies with a uniform size of 200–400 nm, and these particles are fully crystallised. However, the morphology of sample A10 (prepared from α-CrOOH) appears to be irregular, with non-uniform particles that have diameters ranging from 0.3 to 3 μm. It has been shown that the amorphous material was an excellent precursor and offered several advantages over the crystalline precursor [34]. From the experimental data, γ-CrOOH plays a desirable role in regulating crystal growth and produces a Cr_2O_3 pigment with a uniform size, whereas α-CrOOH produces a Cr_2O_3 pigment with non-uniform sizes.

Colour performance is an important characteristic for pigments. The colours of the Cr_2O_3 samples, characterised by $L^*a^*b^*$ coordinates, are provided in Table 1. The commercial Cr_2O_3 pigment (sample P1), which was produced through the reduction of $Na_2Cr_2O_7$ with $(NH_4)_2SO_4$, was chosen as the reference sample. Sample A1 (prepared from γ-CrOOH) presents a brighter yellowish-green colour. Sample A10 (prepared from α-CrOOH) exhibits a significantly less green and darker poor colour.

To increase the diversities in colour performance, Cr_2O_3 samples were prepared by calcining mixtures of α-CrOOH and γ-CrOOH with different compositions. The colour parameters (CIE-$L^*a^*b^*$) are also summarised in Table 1. The value of a^* increases by more than 6 when the content of α-CrOOH increases from 0 to 100 wt%. The value of b^* decreases by more than 8 when the content of α-CrOOH increases from 0 to 100 wt%. The L^* values of all samples are from 51.32 to 48.43, which are very similar to those of the reference sample. This can result in changing colours from bright yellowish-green through bluish-green to brownish green. The significant differences in the colour performance of samples A1, A5, and A10 can be observed in Fig. 6. In addition, the hues of samples A1 to A3 are very similar to that of the commercial Cr_2O_3 pigment sample P1.

It is well known that the intrinsic properties of inorganic pigments are highly affected by their composition, structure, crystallinity, size, and morphology. From the experimental results, Cr_2O_3 with different particle morphologies and sizes are obtained using different precursors. Amorphous γ-CrOOH produces Cr_2O_3 with a uniform size, whereas rhombohedral α-CrOOH produces Cr_2O_3 with non-uniform sizes. The particle morphology and size distribution strongly affect the hue, hiding power, and tinting strength of the pigments [35,36].

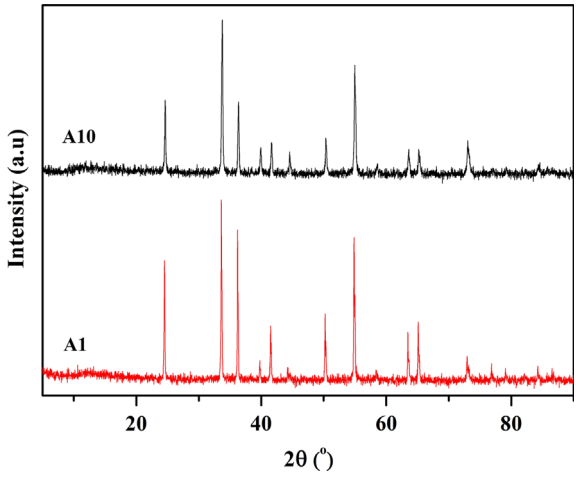

Fig. 4. XRD patterns of samples A1 and A10. A1: Cr_2O_3 prepared from γ-CrOOH; A10: Cr_2O_3 prepared from α-CrOOH.

The colour imparted by Cr_2O_3 pigments is the result of the interaction between the absorption and scattering of light. Chrome oxide has a refractive index of approximately 2.5, which means that a particle size of approximately 300 nm is the ideal primary particle size for Cr_2O_3 pigments to produce optimal tinting strength and scattering power in a standard binder [37,38]. The average particle sizes of Cr_2O_3 prepared from γ-CrOOH are approximately 200–400 nm (Fig. 5(a)), which appear to be identical to the ideal primary particle sizes. Their chromatic coordinates (L^*=50.80, a^*=-18.71, and b^*=20.23) are also excellent. With increasing mean particle sizes, the scattering power decreases more relative to the absorption of the pigment and the obtained colour is darker, bluer, and less saturated [38]. Cr_2O_3 prepared from α-CrOOH has large tabular particles and large sizes; thus, the colours should be a darker bluish green. This phenomenon is consistent with the changes in the $L^*a^*b^*$ values.

The optical properties of Cr^{3+} ions ($3d^3$) in Cr_2O_3 originate from d–d electronic transitions. The optical transitions originate from the strong spin-allowed but parity-forbidden $^4A_{2g} \rightarrow {}^4T_{2g}$

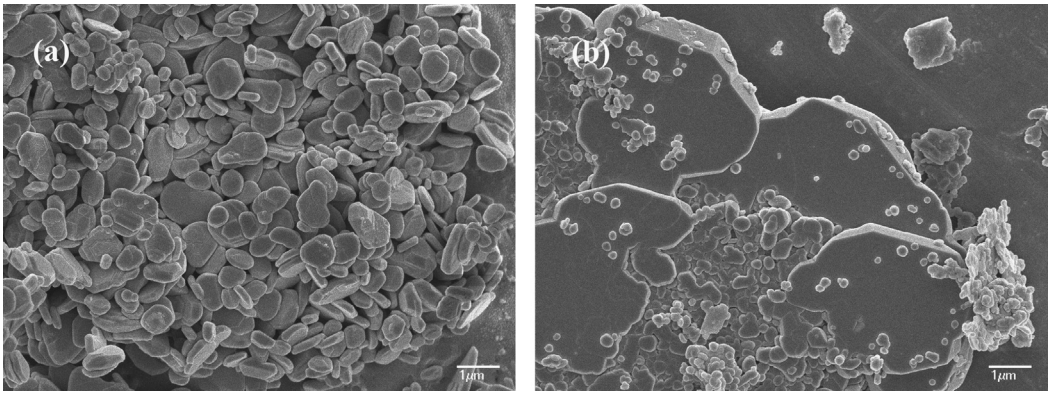

Fig. 5. SEM images of samples A1 and A10: (a) A1: Cr_2O_3 prepared from γ-CrOOH; (b) A10: Cr_2O_3 prepared from α-CrOOH.

Table 1
Chromatic coordinates of Cr_2O_3 pigments (A1–A10) obtained from calcining precursor with different proportions of α-CrOOH and γ-CrOOH at 950 °C for 1.5 h.

Sample	Precursor composition (wt%)		Colour performance			Colour
	α-CrOOH	γ-CrOOH	L^*	a^*	b^*	
A1	0	100	50.12	−18.48	20.20	Yellowish-green
A2	3	97	51.55	−18.40	19.82	Yellowish-green
A3	5	95	51.81	−18.43	19.56	Yellowish-green
A4	7	93	48.43	−17.57	18.08	Bluish-green
A5	10	90	49.12	−16.75	17.27	Green
A6	20	80	49.37	−16.45	17.34	Green
A7	30	70	51.65	−15.99	16.97	Brownish-green
A8	40	60	50.02	−15.04	16.10	Brownish-green
A9	50	50	51.32	−14.42	15.19	Brownish-green
A10	100	0	49.02	−12.07	11.97	Brownish-green
P1	–	–	49.51	−18.00	19.25	Yellowish-green

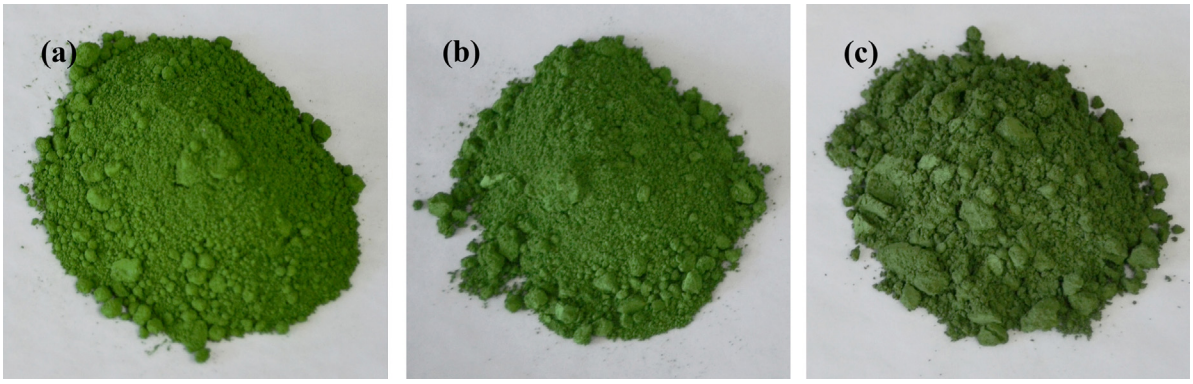

Fig. 6. Photographs of Cr_2O_3 pigments, (a) sample A1, (b) sample A5, and (c) sample A10. Colours of the pigments change from bright yellowish-green (A1) to green (A5) to brownish-green (A10). (For interpretation of the references to colour in this figure legend, the reader is referred to the web version of this article.)

and $^4A_{2g}\rightarrow{}^4T_{1g}$ transitions as well as from the weak spin and parity-forbidden $^4A_{2g}\rightarrow{}^2E_{2g}$ and $^4A_{2g}\rightarrow{}^2T_{1g}$ transitions [15,39,40].

The absorbance curves of the pigments in the UV–vis region are presented in Fig. 7 after subtracting the contribution from the substrate. The absorbance spectra present two well-defined and well-resolved bands in the blue (approximately 460 nm) and yellow (approximately 600 nm) regions of the spectra, respectively. A shoulder in the orange (650–700 nm) regions can also be observed. In fact, a strong absorption feature is observed at 600 nm, most likely originating from the $^4A_{2g}\rightarrow{}^4T_{2g}$ transition of chromium ions in an octahedral environment [41]. The bands at approximately 460 nm can be assigned to the $^4A_{2g}\rightarrow{}^4T_{1g}$ transition of the six-coordinate geometry [11]. Simple nonlinear statistical multi-peak fitting leads to a shoulder centred at 700 nm, attributed to the $^4A_{2g}\rightarrow{}^2T_{1g}$, $^2E_{2g}$ transition [40].

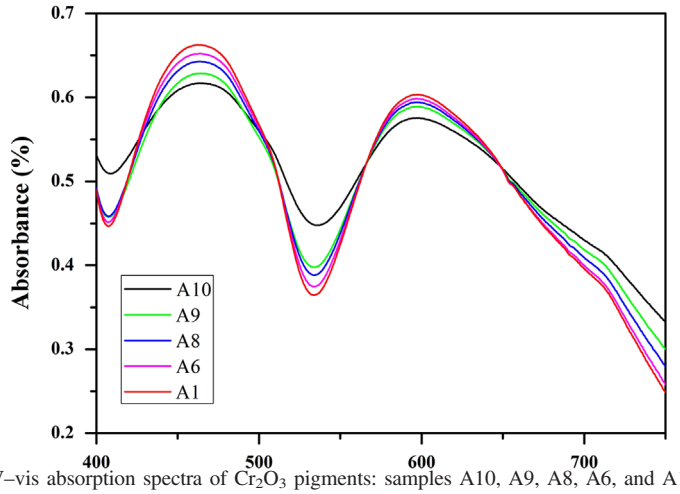

Fig. 7. UV–vis absorption spectra of Cr_2O_3 pigments: samples A10, A9, A8, A6, and A1.

Table 2
Values of Racah parameters *B* and *C* and the energies (*E*) required for electronic transitions of Cr (III) from ground state $^4A_{2g}$.

Sample	Precursor composition (wt%)		E ($^4T_{1g}$)	E ($^4T_{1g}$) = 10Dq	E ($^2T_{1g}$)	E (^4E_g)	B	C
	α-CrOOH	γ-CrOOH						
A1	0	100	16648	21,645	14780	–	466	3527
A6	20	80	16636	21,667	14799	–	470	3522
A8	40	60	16604	21,667	14740	–	474	3492
A9	50	50	16694	21,669	14644	–	464	3490
A10	100	0	16696	21,706	14616	–	468	3469

A gradual shift of these bands can be observed with variations of γ-CrOOH and α-CrOOH in the precursors.

Deconvolution of the UV–vis spectra of the Cr_2O_3 pigments was conducted, and the results are presented in Table 2. The energy of the spin-allowed $^4A_{2g} \rightarrow {}^4T_{1g}$ transition varies between 21,706 and 21,645 cm^{-1} according to the change of α-CrOOH and γ-CrOOH. The absorption peaks are red-shifted, showing increases in the b^* value. The energy of the spin-forbidden $^4A_{2g} \rightarrow {}^2T_{2g}$ transition presents little variation. This energy shifted from 147616 cm^{-1} in sample A10 to 14780 cm^{-1} in sample A1. A red-shift in the spectra occurs for sample A1. Red colour is absorbed, and a complimentary bright green colour appears.

4. Conclusion

Through the hydrogen reduction of K_2CrO_4, two different types of CrOOH, γ-CrOOH and α-CrOOH, were prepared. Amorphous γ-CrOOH produces more homogeneous Cr_2O_3 with a uniform size of 200–400 nm and a yellowish-green colour. Rhombohedral α-CrOOH produces Cr_2O_3 with non-uniform sizes and a brownish-green colour. By changing the proportions of α-CrOOH and γ-CrOOH in the precursor, the resulting pigments can exhibit a variety of controllable colours, including bright yellowish-green, bluish-green, green, and brownish-green.

Furthermore, the different precursors (i.e., γ-CrOOH and α-CrOOH) may affect the particle morphologies, sizes, and the crystal field of the Cr_2O_3 pigment, thus affecting the final greenish colouration. When the Cr_2O_3 green pigment is prepared from γ-CrOOH rather than α-CrOOH, a red-shift of the absorption peaks resulting from the $^4A_{2g} \rightarrow {}^4T_{1g}$ transition occurs, which helps to increase the b^* value. The red-shift of the absorption peaks due to the $^4A_{2g} \rightarrow {}^2T_{2g}$ transition might also be helpful to improve the $-a^*$ value.

Acknowledgements

The authors gratefully acknowledge the financial support from the National Natural Science Foundation of China (No. 50904058) and the National High-tech Research and Development Programme of China (No. 2011AA060702).

References

[1] K.H. Büchel, H.H. Moretto, D. Werner, Industrial Inorganic Chemistry, Wiley-Vch, Germany, 2008.
[2] William W. Carlin, Preparation of pigmentary chromic oxide, US Patent 4,127,643, 1978.
[3] R. Aghababazadeh, A. Mirhabibi, F. Moztarzadeh, Z. Salehpour, Synthesis and characterisation of chromium oxide as a pigment for high temperature application, Pigment & Resin Technology 32 (3) (2003) 160–165.
[4] T. Tsuzuki, P.G. McCormick, Synthesis of Cr_2O_3 nanoparticles by mechanochemical processing, Acta Materialia 48 (11) (2000) 2795–2801.
[5] V.P. Rao, Preparation of pigment grade chromium oxide, EP Patent 0,068,787, 1984.
[6] V. Wilhelm, D. Messer, Process for the preparation of pigments containing Cr_2O_3, US Patent 5,167,708, 1992.

[7] B. Knickel, S. Keifer, H. Perrey, H. Rudolph, H.J. Rosenkranz, R. Rudisch, Modified chromium oxide pigment, US Patent 3,960,590, 1976.
[8] P. Li, H.-B. Xu, Y. Zhang, Z.-H. Li, S.-L. Zheng, Y.-L. Bai, The effects of Al and Ba on the colour performance of chromic oxide green pigment, Dyes and Pigments 80 (3) (2009) 287–291.
[9] T. Thongkanluang, T. Kittiauchawal, P. Limsuwan, Preparation and characterization of Cr_2O_3–TiO_2–Al_2O_3–V_2O_5 green pigment, Ceramics International 37 (2) (2011) 543–548.
[10] T. Thongkanluang, P. Limsuwan, P. Rakkwamsuk, Preparation and application of high near-infrared reflective green pigment for ceramic tile roofs, International Journal of Applied Ceramic Technology 8 (6) (2011) 1451–1458.
[11] S. Sangeetha, R. Basha, K.J. Sreeram, S.N. Sangilimuthu, B. Unni Nair, Functional pigments from chromium(III) oxide nanoparticles, Dyes and Pigments 94 (3) (2012) 548–552.
[12] S.A. Eliziário, J.M. de Andrade, S.J.G. Lima, C.A. Paskocimas, L.E. B. Soledade, P. Hammer, et al., Black and green pigments based on chromium–cobalt spinels, Materials Chemistry and Physics 129 (1–2) (2011) 619–624.
[13] F.J. Berry, N. Costantini, L.E. Smart, Synthesis of chromium-containing pigments from chromium recovered from leather waste, Waste Management 22 (7) (2002) 761–772.
[14] E. Ozel, S. Turan, Production and characterisation of iron-chromium pigments and their interactions with transparent glazes, Journal of the European Ceramic Society 23 (12) (2003) 2097–2104.
[15] R.S. Pavlov, V.B. Marzá, J.B. Carda, Electronic absorption spectroscopy and colour of chromium-doped solids, Journal of Materials Chemistry 12 (9) (2002) 2825–2832.
[16] D. Duranoğlu, İ.G. Buyruklardan Kaya, U. Beker, B.F. Şenkal, Synthesis and adsorption properties of polymeric and polymer-based hybrid adsorbent for hexavalent chromium removal, Chemical Engineering Journal 181–182 (2012) 103–112.
[17] V.M. Boddu, K. Abburi, J.L. Talbott, E.D. Smith, Removal of hexavalent chromium from wastewater using a new composite chitosan biosorbent, Environmental Science & Technology 37 (19) (2003) 4449–4456.
[18] H.-B. Xu, Y. Zhang, Z.-H. Li, S.-L. Zheng, Z.-K. Wang, T. Qi, et al., Development of a new cleaner production process for producing chromic oxide from chromite ore, Journal of Cleaner Production 14 (2) (2006) 211–219.
[19] Y. Zhang, Z.-H. Li, T. Qi, S.-L. Zheng, H.-Q. Li, H.-B. Xu, Green manufacturing process of chromium compounds, Environmental Progress 24 (1) (2005) 44–50.
[20] S. Zheng, Y. Zhang, Z. Li, T. Qi, H. Li, H. Xu, Green metallurgical processing of chromite, Hydrometallurgy 82 (3–4) (2006) 157–163.
[21] Y.-L. Bai, H.-B. Xu, Y. Zhang, Z.-H. Li, Reductive conversion of hexavalent chromium in the preparation of ultra-fine chromia powder, Journal of Physics and Chemistry of Solids 67 (12) (2006) 2589–2595.
[22] P. Li, H.-B. Xu, S.-L. Zheng, Y. Zhang, Z.-H. Li, Y.-L.A. Bai, Green process to prepare chromic oxide green pigment, Environmental Science & Technology 42 (19) (2008) 7231–7235.
[23] S. Kittaka, T. Morooka, K. Kitayama, T. Morimoto, Thermal decomposition of chromium oxide hydroxide: I. Effect of particle size and atmosphere, Journal of Solid State Chemistry 58 (2) (1985) 187–193.
[24] M. Maciejewski, K. Köhler, H. Schneider, A. Baiker, Interconversion of CrO_2 formed by decomposition of chromium(III) nitrate nonahydrate, Journal of Solid State Chemistry 119 (1) (1995) 13–23.
[25] J. Yang, H. Cheng, W.N. Martens, R.L. Frost, Transition of synthetic chromium oxide gel to crystalline chromium oxide: a hot-stage Raman spectroscopic study, Journal of Raman Spectroscopy 42 (5) (2011) 1069–1074.
[26] J. Yang, A. Baker, H. Liu, W. Martens, R. Frost, Size-controllable synthesis of chromium oxyhydroxide nanomaterials using a soft chemical hydrothermal route, Journal of materials science 45 (24) (2010) 6574–6585.
[27] A.N. Christensen, Hydrothermal preparation and magnetic-properties of alpha-CrOOH, beta-CrOOH, and gamma-CrOOH, Acta Chemica Scandinavica Series A—Physical and Inorganic Chemistry 30 (2) (1976) 133–136.
[28] A.n. Christen, Crystal structure of a new polymorph of CrOOH, Inorganic Chemistry 5 (8) (1966) 1452–1453.
[29] N.C. Tombs, W.J. Croft, J.R. Carter, J.F.A. Fitzgerald, New polymorph of CrOOH, Inorganic Chemistry 3 (12) (1964) 1791–1792.
[30] A. Shpachenko, N. Sorokhtina, N. Chukanov, A. Gorshkov, A. Sivtsov, Genesis and compositional characteristics of natural γ-CrOOH, Geochemistry International 44 (7) (2006) 681–689.
[31] J. Yang, W.N. Martens, R.L. Frost, Transition of chromium oxyhydroxide nanomaterials to chromium oxide: a hot-stage Raman spectroscopic study, Journal of Raman Spectroscopy 42 (5) (2011) 1142–1146.
[32] S. Kittaka, T. Tahara, Thermal decomposition of chromium oxide hydroxide: II. Texture change of α-$HCrO_2$ through thermal decomposition under vacuum, Journal of Colloid and Interface Science 112 (1) (1986) 252–260.
[33] S. Kittaka, R. Fujinaga, K. Morishige, T. Morimoto, Adsorption of water on the surfaces of α-$HCrO_2$ and Cr_2O_3, Journal of Colloid and Interface Science 102 (2) (1984) 453–461.
[34] I.J. Clark, T. Takeuchi, N. Ohtori, D.C. Sinclair, Hydrothermal synthesis and characterisation of $BaTiO_3$ fine powders: precursors, polymorphism and properties, Journal of Materials Chemistry 9 (1) (1999) 83–91.
[35] G. Buxbaum, Industrial Inorganic Pigments, Wiley-Vch, Germany, 2008.
[36] K. Bittler, W. Ostertag, Developments in the field of inorganic pigments, Angewandte Chemie International Edition in English 19 (3) (1980) 190–196.
[37] P.J. Cao, H.D. Wu, J.L. Dong, Research on application of nano-TiO_2 in automotive coating, Applied Mechanics and Materials 160 (2012) 216–222.
[38] ⟨http://www.rpigments.com/Tech?color=4&type=&form=&application=&region=⟩.
[39] S. Sugano, Y. Tanabe, H. Kamimura, Multiplets of Transition-Metal Ions in Crystals, Academic Press, New York, 1970.
[40] L. Vayssieres, A. Manthiram, 2-D Mesoparticulate arrays of α-Cr_2O_3, Journal of Physical Chemistry B. 107 (12) (2003) 2623–2625.
[41] É. Gaudry, P. Sainctavit, F. Juillot, F. Bondioli, P. Ohresser, I. Letard, From the green color of eskolaite to the red color of ruby: an X-ray absorption spectroscopy study, Physics and Chemistry of Minerals 32 (10) (2006) 710–720.